The surface curvature effect on performance of a laboratory scale tidal turbine

Kaiming Ai, Eldad Avital, *Member, IAENG,*, Xiang Shen, Abdus Samad, Nithya Venkatesan

***Abstract*—This paper presents numerical study of the surface curvature effects on the performance of a 3D lab scale tidal turbine (E387) using Eppler 387 airfoil. The prescribed surface curvature distribution blade design method is used to remove the surface curvature discontinuity of E387 turbine and the redesigned turbine is denoted as A7 turbine. The two turbines are analysed using in-house BEM code and CFD RANS. The performance of E3787 turbine obtained from BEM and RANS match well with the experimental results from reported literature. The A7 turbine has mildly better performance at low tip speed ratio (1-4.25) at which the blade is partly or fully stalled.**

***Index Terms*—surface curvature effect, CIRCLE, tidal turbine, power coefficient, BEM**

I. Introduction

ACCORDING to the recent REN21 report [1], 19.3% of global energy comes from renewable energy in 2015, in which modern renewable energy constituted nearly 10.2%, and hydropower made up about 3.6%. Among those renewable resources, one of the most promising energy is tidal power. One advantage of the tidal turbine is that it doesn't need to build dam like traditional hydropower.

A tidal turbine blade is composed of profiles located along the span. The performance of tidal turbine is determined by several parameters such as the fluid property, tip speed ratio(TSR), blade shape and diameter. The blade design process normally involves proper parameters such as the airfoil shape at different station, twist angle, and chord length. For stall regulated tidal turbine,the operational TSR of tidal turbine changes due to the variation of inflow tidal current and wave speed, thus the tidal turbine operates at off-design TSR at most cases. In order to capture more power, it is important to maintain a relative high power coefficient at a wide range of TSR.

For wall bounded flow, the boundary layer starts from the leading edge of the profile and develops towards the trailing edge. The leading edge shape plays an important role in the start of boundary layer and affects the development of boundary layer at the blade surface[2].

The surface curvature discontinuity of the airfoil or blades has been realized in references [3] [4] [5]. Song et al removed the surface discontinuity at leading edge and main surface of a compressor blade respectively, and found that smoothing the leading edge has better performance than its main surface counterpart [3]. The surface curvature of NREL S814 airfoil was smoothed using prescribed surface curvature distribution blade design (CIRCLE) method and renamed as R1, the RANS results show that the R1 has lower lift and drag but higher lift to drag coefficients at $Re = 1.5 \times 10^6$ with angle of attack varies from 3-11 degree[6].

The prescribed surface curvature distribution blade design (CIRCLE) method was originally proposed by Korakianitis and applied to axial turbomachinery cascades [7]. The CIRCLE method redesigns the blade profile coordinates to yield a continuous curvature and slope of curvature, thus a smooth pressure and velocity distributes along the blade surface. Korakianitis applied the CIRCLE method to various blades [8] and airfoils [6] .

Later shen et al [9] further extended Korakianitis' work. Shen conducted experimental and numerical study of Eppler 387 and redesigned A7 airfoil at three different Reynolds number (1×10^5, 2×10^5 and 3×10^5) . Shen et al concluded that removing the surface curvature discontinuity increases the aerodynamic performance and reduces drag of airfoil at high angle of attack (AOA) and stall condition. Shen et al also compared the performance of 3KW small turbines whose rotors are composed of E387 and A7 airfoils respectively. The steady Blade Element Momentum results showed that the A7 had noticeable improvement of power coefficient at low tip speed ratio (TSR), and marginal improvement at optimal and large tip speed ratio.

The aforementioned research only analysed the surface curvature effects on performance for 2D isolated airfoil, turbine cascades using numerical or experimental methods. Shen et al [9] studied the performance improvement of a 3D wind turbine model by replacing E387 airfoil with redesigned A7 airfoil at all blade stations using a simple method like BEM, but have not explain the mechanism of improved power coefficient at small tip speed ratio. Also, the power performance obtained from BEM has not been validated by comparing with experimental data. To have a better understand the mechanism, more advanced methods such as CFD can be used to analysis the fluid field of a rotating blade.

The purpose of this study is to analysis the flow field and the performance improvement of tidal turbine optimization based on CIRCLE methods. The BEM methods and CFD are used to analysis the total performance and spanwise distribution of local angle of attack, streamline, lift to drag ratio of the E387 turbine [10] and redesigned A7 turbine at different operation conditions.

II. Blade redesign and Numerical Modelling

A. Blade Geometry

A laboratory scale turbine model [10] (denoted as E387 turbine)has been chosen for this study cause the turbine

Manuscript received March 05, 2018; revised April, 18, 2018

K.Ai, E. Avital and X. Shen are with School of Engineering and Materials Science, Queen Mary University of London, UK email: k.ai@qmul.ac.uk, e.avital@qmul.ac.uk, x.shen@qmul.ac.uk

A. Samad is with Ocean Engineering, IIT Madras, India, email: samad@iitm.ac.in

N. Venkatesan is with Electric Engineering, VIT Chennai, India, email: nithya.v@vit.ac.in

model is composed of Eppler 387 profile which has been redesigned using the CIRCLE method [9]. The diameter of the turbine is 0.46m. At the tip station, the pitch angle is 0 degree and chord length is 25mm. The root station is located at 0.1R with local pitch angle 20 degree and chord length of 50mm. The chord length and twist angle are assumed to vary linearly between the tip and root station. The diameter of the nacelle is 66mm, which extends 60mm upstream and downstream and attaches to the hemisphere cone.The CAD turbine model (Fig. 1) is created with Solidworks ®.

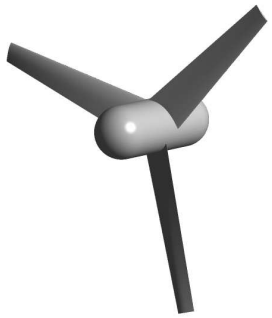

Fig. 1: Blade and nacelle

B. Turbine Redesign

The surface discontinuity of the E387 airfoil is removed using the CIRCLE method [11], [12]. The redesigned airfoil is named A7. The coordinate and curvature distribution of E387 and A7 airfoils are presented in Fig. 2 and Fig. 3

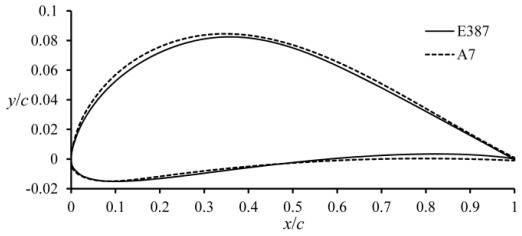

Fig. 2: Coordinates of E387 and A7 [9]

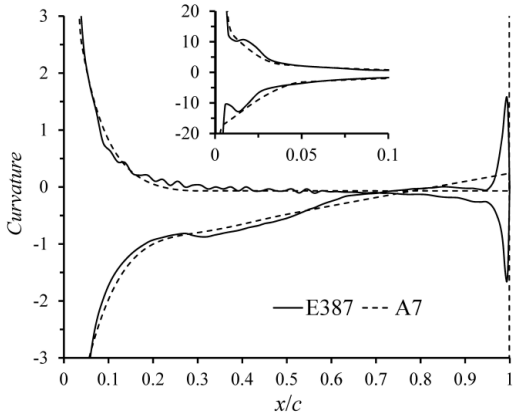

Fig. 3: Curvature distribution of E387 and A7 [9]

A redesigned A7 turbine is obtained by replacing the original E387 airfoil at each blade station while keeping all other parameters the same.

C. Numerical Modelling Methods

The E387 profile is designed as a sharp trailing edge.The shape trailing edge is un-physical in experimental model and leads to skewed mesh in numerical modelling. Normally there are two methods to deal with sharp trailing edge. One method is to simply cut the trailing edge, which decreases the chord length and changes the thickness to chord length ratio. Another better method is to thicken the trailing edge. Thickened trailing edge keeps the ratio of thickness to chord length. Thickened trailing edge method has been adopted in the experimental airfoil model, such as [13] [14]. The trailing edge thickness is normally about 0.1%c. The method used in NASA experimental model [13] has been adopted in the paper. The E387 coordinates has been thickened between 0.95-1c with a blunt trailing edge of 0.1%c.

The steady Blade Element Momentum (BEM) method and CFD are used to analysis the performance of E387 and A7 turbine. In BEM code ,the 2D aerodynamic parameters (Cl, Cd) of airfoils at $Re = 1 \times 10^5$ are from experimental data [13][9] and then extrapolated using AirfoilPrep [15].

The computational domain is shown in Figure 5. Periodic boundary condition is used to reduce the computational resources. The origin of coordinate is located at the centre of rotational plane.The inlet is located 3 diameter (D) upstream of rotor, and the outlet is 6D downstream, the radial distance is 2.5D.

The inlet boundary is specified as velocity inlet at 0.6m/s at all cases, while the TSR is obtained by changing the rotational speed of the rotor. The outlet is specified as pressure outlet with a pressure of 1 atm. the circumference is set as symmetry boundary condition, and the sides are set as periodic boundaries. The Moving Reference Frame is used to account for the rotor rotating[16]. The fluid field is assumed to be one phase (water), free surface and bed isn't considered in this simulation. The TSR varies from 1 to 8, and the corresponding Reynolds number is $4.5 \times 10^4 - 1.8 \times 10^5$ based on relative speed and chord lenth at 0.5R. The prism and tetra mesh (Figure 6) are used in this study The prism layers are used in the blade surface to capture the boundary layer properties. Four different mesh sizes are used to study the mesh independence (Figure 4), which shows that the grid converges at mesh size of 15 million with a y plus value is below 2.

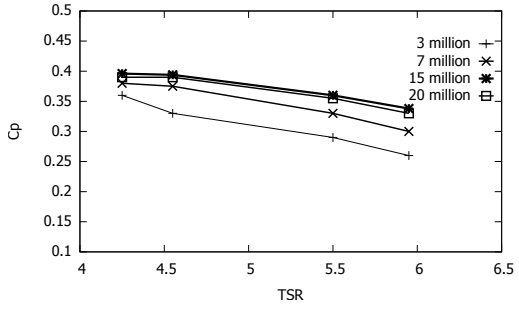

Fig. 4: Grid convergence of E387

References [17] [18]show that Steady RANS and the $k-\omega$ SST turbulence model are appropriate for this simulation. ANSYS Fluent is used for the numerical simulation which runs on Apocrita cluster at QMUL. The residuals drop below

$10-5$ after about 3000 iterations which take 2.5-3 hours using 64 cores parallel running.

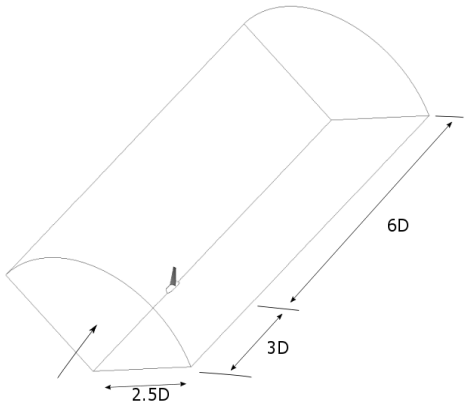

Fig. 5: Computational domain

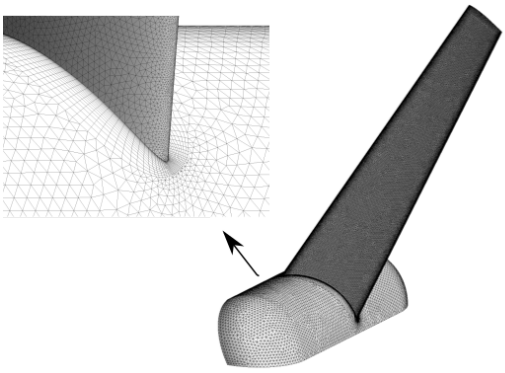

Fig. 6: blade and nacelle mesh

The governing equations are Reynolds Averaged Navier-Stokes equations which are defined as:

$$\frac{\partial U_i}{\partial x_i} = 0 \tag{1}$$

$$\frac{\partial U_i}{\partial t} + \frac{\partial (U_i U_j)}{\partial x_j} = -\frac{1}{\rho}\frac{\partial P}{\partial x_i} + \frac{\partial}{\partial x_j}(\nu \frac{\partial U_i}{\partial x_j} - \overline{u_i u_j}) \tag{2}$$

The main parameters for tidal turbine performance analysis are tip speed ratio, power and thrust coefficients, which are defined as:

$$TSR = \frac{\omega R}{U_\infty} \tag{3}$$

$$C_p = \frac{P}{\frac{1}{2}\rho A U_\infty^3} \tag{4}$$

$$C_T = \frac{T}{\frac{1}{2}\rho A U_\infty^2} \tag{5}$$

III. Results and Discussion

The variation of the power coefficient, Cp, with the TSR is shown in Figure 7. Good agreement is observed between BEM, RANS and the experimental result conducted by Luznik et al [10]. When compared with the Cp from RANS, the power coefficient from BEM mildly overshoots near the optimal TSR. The BEM and RANS results show that the redesigned A7 turbine has noticeable better power performance at low TSR (1-4.25). From the RANS result, the power coefficient of the A7 turbine increased 5.5% at TSR 3.5. The improvement of Cp at low TSR can be explained after analysing the local angle of attack distribution along the spanwise direction at different TSR.

The optimal TSR is the TSR value where the max power coefficient is obtained. For E387 turbine, the optimal TSR is 4.25. Experimental results show that the E387 airfoil starts to stall when the AOA is higher than 8 degree at $Re = 1 \times 10^5$ [14] . When TSR is 4.25, the local angle of attack is stalled near the blad root ($r < 0.3R$) (8). When the operational TSR is below 4.25, the main body of the blade start to stall and the sectional lift decreases and drag increases dramatically. As the rotational speed decreases, the TSR decreases as well, which leads to the increase of the effective angle of attack, thus the blade stalls. The A7 turbine has marginally higher power coefficient compared to original E387 turbine due to the stall delay offered by the A7 profile.

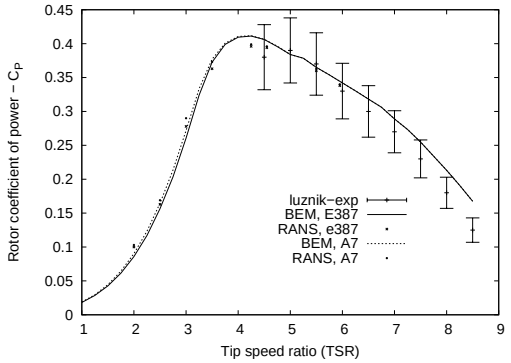

Fig. 7: the power coefficient versus TSR

The local angle of attack along spanwise direction is shown in Figure 8. At a fixed spanwise location, the local angle of attack decreases as the increase of TSR. Similarly, at a fixed TSR, the local angle of attack has highest value at root station and decreases towards the blade tip. The local angle of attack at all stations are stalled when the TSR is below 3. Figure 9 shows the local angle of attack of E387 and A7 turbine at TSR =3.25. The angle of attacks of E387 and A7 turbine are the same, and the blades are stalled except towards the tip.

The lift to drag ratio is an important parameter for choosing the right airfoil shape of tidal turbine. The lift to drag ratio increases exponentially from root to tip (Figure 10). The A7 turbine has better hydrodynamic efficiency around stall condition due to the delay in stall.

The local streamlines of E387 at three blade stations are shown in Figure 12 11. A vortex exists at leading ledge at 0.2R when the rotor operates at TSR =3.

The limit streamlines of E387's suction surface at three different TSRs are shown in Figure 13. For TSR =5, the flow is mainly attached to the suction side of the blade except the root region. At TSR= 4.25, the flow separation starts from the trailing edge at the middle-span location. Figure 14 show the suction limit streamlines of E387 and A7 at TSR 4.25. In both cases, the flow are attached to the blade surface in the main and tip regions but stalled near the hub

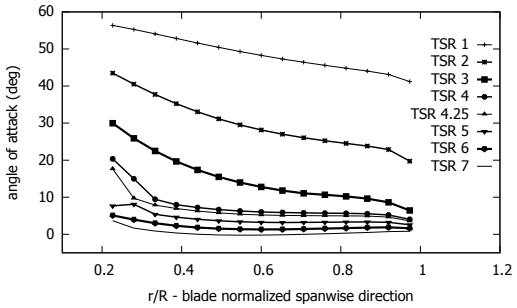

Fig. 8: Local angle of attack distribution along spanwise direction, E387 turbine

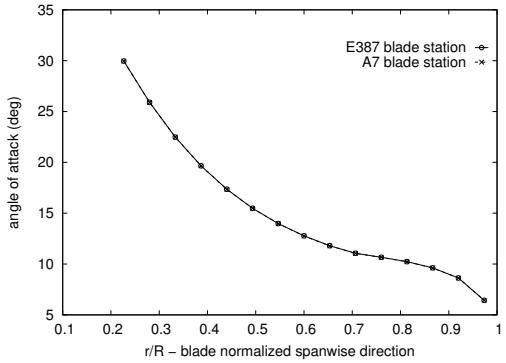

Fig. 9: AOA at TSR 3.25

region. A noticeable difference of the limit streamline pattern is observed near the blade root, where the limit streamline pattern of A7 moves closer to the trailing edge.

IV. Conclusion

The flow field of the E387 and A7 turbine are analysed using CFD and BEM method. The optimal TSR for the lab turbine model is about 4.25, at which the flow is attached to the blade suface in the middle-span, but separated when the spanwise distance form the axis is below 0.4r/R. The numerical analysis of the flow field of E387 turbine provides insights for further blade design optimization. The original E387 turbine has been optimized using CIRCLE method. The BEM and RANS results show that the surface continuous redesigned A7 turbine has mildly better power performance at low tip speed ratio, which imply the continuous curvature blade can used a method for stall delay.

Acknowledgment

The first author would like to thank the Queen Mary China Scholarship Council Co-funded Scholarships. This research utilised Queen Mary's Apocrita HPC facility, supported by QMUL Research-IT. http://doi.org/10.5281/zenodo.438045

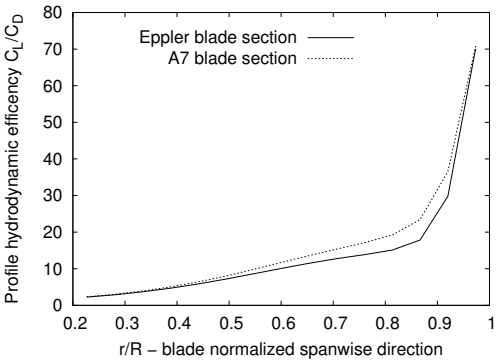

Fig. 10: the hydrodynamic efficiency along spanwise direction (TSR 3.25)

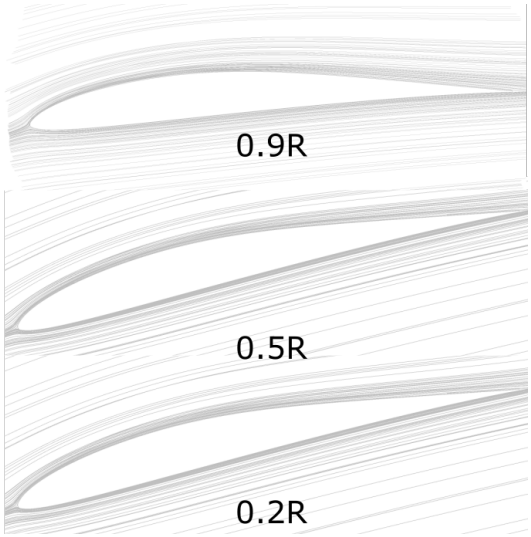

Fig. 11: Local steamline of E387 at TSR 5.5 (rotational frame, chord lengthes are scaled)

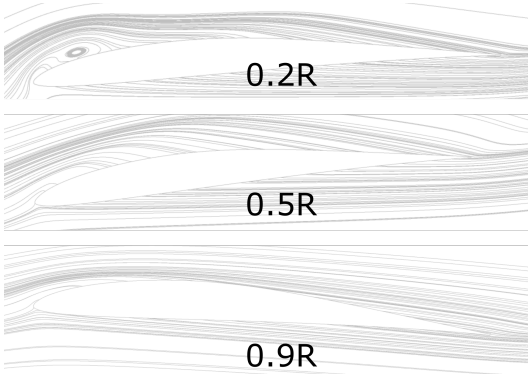

Fig. 12: Local steamline of E387 at TSR 3 (rotational frame, chord lengthes are scaled)

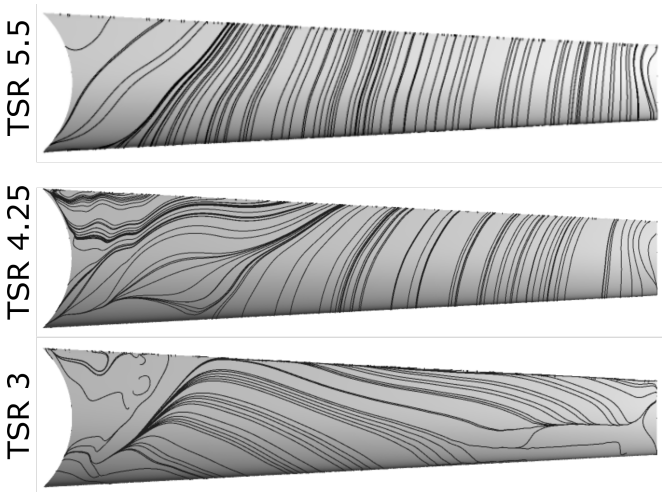

Fig. 13: Blade limit streamline E387(flow direction from bottom to top)

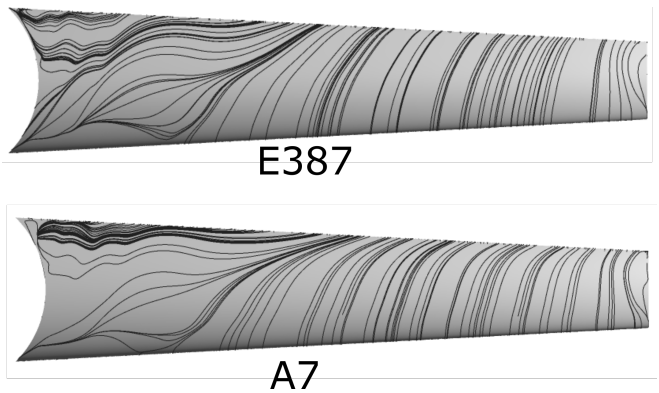

Fig. 14: Blade limit streamline, TSR, 4.25

REFERENCES

[1] C. Lins, E. Musolino, K. Petrichenko, W. Rickerson, J. Sawin, K. Seyboth, J. Skeen, B. Sovacool, F. Sverrisson, and L. Williamson, "Renewables 2017 global status report," 2017.

[2] H. Hodson, "Boundary-layer transition and separation near the leading edge of a high-speed turbine blade," *Journal of Engineering for Gas Turbines and Power*, vol. 107, no. 1, pp. 127–134, 1985.

[3] Y. Song, C.-W. Gu, and Y.-B. Xiao, "Numerical and theoretical investigations concerning the continuous-surface-curvature effect in compressor blades," *Energies*, vol. 7, no. 12, pp. 8150–8177, 2014.

[4] T. Korakianitis, I. Hamakhan, M. Rezaienia, A. Wheeler, E. Avital, and J. Williams, "Design of high-efficiency turbomachinery blades for energy conversion devices with the three-dimensional prescribed surface curvature distribution blade design (circle) method," *applied Energy*, vol. 89, no. 1, pp. 215–227, 2012.

[5] T. Korakianitis, M. Rezaienia, I. Hamakhan, and A. Wheeler, "Two- and three-dimensional prescribed surface curvature distribution blade design (circle) method for the design of high efficiency turbines, compressors, and isolated airfoils," *Journal of Turbomachinery*, vol. 135, no. 4, p. 041002, 2013.

[6] T. Korakianitis, M. Rezaienia, I. Hamakhan, E. Avital, and J. Williams, "Aerodynamic improvements of wind-turbine airfoil geometries with the prescribed surface curvature distribution blade design (circle) method," *Journal of engineering for gas turbines and power*, vol. 134, no. 8, p. 082601, 2012.

[7] T. Korakianitis, "Hierarchical development of three direct-design methods for two-dimensional axial-turbomachinery cascades," *Journal of turbomachinery*, vol. 115, no. 2, pp. 314–324, 1993.

[8] I. Hamakhan and T. Korakianitis, "Aerodynamic performance effects of leading-edge geometry in gas-turbine blades," *Applied Energy*, vol. 87, no. 5, pp. 1591–1601, 2010.

[9] X. Shen, E. Avital, G. Paul, M. A. Rezaienia, P. Wen, and T. Korakianitis, "Experimental study of surface curvature effects on aerodynamic performance of a low reynolds number airfoil for use in small wind turbines," *Journal of Renewable and Sustainable Energy*, vol. 8, no. 5, p. 053303, 2016.

[10] L. Luznik, K. A. Flack, E. E. Lust, and K. Taylor, "The effect of surface waves on the performance characteristics of a model tidal turbine," *Renewable energy*, vol. 58, pp. 108–114, 2013.

[11] M. Ahmed, E. Avital, and T. Korakianitis, "Investigation of improved aerodynamic performance of isolated airfoils using circle method," *Procedia Engineering*, vol. 56, pp. 560–567, 2013.

[12] X. Shen, T. Korakianitis, and E. Avital, "Numerical investigation of surface curvature effects on aerofoil aerodynamic performance," in *Applied Mechanics and Materials*, vol. 798. Trans Tech Publ, 2015, pp. 589–595.

[13] R. J. McGhee, B. S. Walker, and B. F. Millard, "Experimental results for the eppler 387 airfoil at low reynolds numbers in the langley low-turbulence pressure tunnel," 1988.

[14] M. S. Selig and B. D. McGranahan, "Wind tunnel aerodynamic tests of six airfoils for use on small wind turbines; period of performance: October 31, 2002–january 31, 2003," National Renewable Energy Laboratory (NREL), Golden, CO., Tech. Rep., 2004.

[15] S. Ning, "Airfoilprep. py documentation: Release 0.1. 0," National Renewable Energy Lab.(NREL), Golden, CO (United States), Tech. Rep., 2013.

[16] A. Fluent, "18.0 ansys fluent theory guide 18.0," *Ansys Inc*, 2017.

[17] M. Rahimian, J. Walker, and I. Penesis, "Numerical assessment of a horizontal axis marine current turbine performance," *International Journal of Marine Energy*, vol. 20, pp. 151–164, 2017.

[18] T. Karthikeyan, E. Avital, N. Venkatesan, and A. Samad, "Design and analysis of a marine current turbine," in *ASME 2017 Gas Turbine India Conference*. American Society of Mechanical Engineers, 2017, pp. V001T02A014–V001T02A014.